UNIVERSIDAD NACIONAL DE COLOMBIA
SEDE MEDELLÍN
FACULTAD DE MINAS

DYNA
http://dyna.medellin.unal.edu.co/

Occurrence of a skarn-type mineralogy found in Ciénaga Marbles, located in the NW foothills of the Santa Marta Massif (Colombia)

Oscar Mauricio Castellanos-Alarcón [a], Carlos Alberto Ríos-Reyes [b] & Luis Carlos Mantilla-Figueroa [b]

[a] *Programa de Geología, Universidad de Pamplona, Pamplona, Colombia, oscarmca@yahoo.es*
[b] *Escuela de Geología, Universidad Industrial de Santander, Bucaramanga, Colombia, carios@uis.edu.co*
[b] *Escuela de Geología, Universidad Industrial de Santander, Bucaramanga, Colombia, lcmantil@uis.edu.co*

Received: September 3rd, 2014.Received in revised form: August 4th, 2015.Accepted: September 20th, 2015.

Abstract
The early Cretaceous Ciénaga Marbles that crop out in the NW foothills of the Santa Marta Massif (Colombian Caribbean region) present an epigenetic mineral assemblage (skarn-type), overprinting the metamorphic mineral assemblage previously developed along the regional metamorphic history that affected this unit. The skarn-type mineralogy allows at least three paragenetic contexts to be distinguished, which are represented by the following neoformed minerals: (a) garnet, forsterite, diopside, titanite, wollastonite and calcite (early anhydrous metamorphic stage), (b) actinolite, tremolite, allanite and clinohumite (metasomatic or hydrated stage), and (c) chlorite, serpentine, sepiolite and quartz (late low temperature retrograde stage, probably due to infiltration of descending meteoric waters). The skarn-type mineralogy is observed as alteration halos developed around porphyritic granodiorites emplaced as sills between anisotropy planes related to metamorphic regional foliation of rock that are considered to be the causative bodies of the skarn-type mineralogy. Zircon U-Pb ages obtained from granodioritic bodies yielded an age of 55.5±0.7 Ma (Ypresian, Early Eocene). The formation of the skarn-type mineralogy in the Ciénaga Marbles is temporarily related to the formation and emplacement of hydrated silicate masses that were generated at the beginning of the subduction polarity change (*i.e.* when the Caribbean oceanic plate began to subduct beneath South American continental plate).

Keywords: Ciénaga Marbles; Santa Marta massif; skarn-type mineralogy; zircon U-Pb geochronology; Caribbean Plate.

Ocurrencia de una mineralogía tipo skarn reconocida en los Mármoles de Ciénaga, estribaciones NW del Macizo de Santa Marta (Colombia)

Resumen
Los Mármoles de Ciénaga del Cretácico Temprano que afloran en las estribaciones NW del Macizo de Santa Martha (región del Caribe Colombiano) presentan una asociación mineral epigenética de tipo skarn, sobreimpuesta a la asociación mineral formada previamente durante la historia de metamorfismo regional que afectó a esta unidad. La mineralogía tipo skarn permitió diferenciar al menos tres contextos paragenéticos, representados por los siguientes minerales: (a) granate, forsterita, diópsido, titanita, wollastonita y calcita (etapa metamórfica anhidra temprana), (b) actinolita, tremolita, clinonohimita y allanita (etapa metasomática o hidratada), y (c) clorita, serpentina, sepiolita y cuarzo (etapa retrógrada de baja temperatura tardía probablemente debido a infiltración descendente de aguas meteóricas). La mineralogía tipo skarn suele desarrollarse a manera de halos de alteración entorno a granodioritas porfiríticas emplazadas como *sills* entre los planos de la foliación regional de las rocas metamórficas, los cuales se consideran como los cuerpos causativos de la mineralogía tipo skarn. Dataciones U-Pb en circones de éstos cuerpos granodioríticos produjeron una edad de 55.5±0.7 Ma (Ypresiano, Eoceno Temprano). La formación de la mineralogía tipo skarn en los Mármoles de Ciénaga se relaciona temporalmente con la formación y el emplazamiento de masas silicatadas hidratadas, generadas al inicio del cambio en la polaridad de la subducción (es decir, cuando la placa oceánica del Caribe comenzó a subducir por debajo de la placa continental sudamericana).

Palabras clave: Mármoles de Ciénaga; Macizo de Santa Marta; Mineralogía tipo Skarn; Geocronología U-Pb en circones; Placa Caribe.

1. Introduction

A skarn-type mineralogy may be formed during regional or contact metamorphism and from a variety of metasomatic processes involving a great variety of fluids (magmatic, metamorphic, meteoric, and/or marine in origin). This mineral assemblage is characterized by the presence of calc-silicate minerals (e.g. garnet and pyroxene), among others

minerals [1-3]. The recognition of a skarn-type mineralogy is very relevant in terms of mineral exploration because of its relationship with mineral deposits formation [4-15]. The major part of skarn-type mineralogy can be related to causative igneous rocks emplaced at various tectonic settings [3]. The most economic skarn deposits are related to metasomatic processes that affect the country rocks (e.g. marbles) that are used to host hydrated silicate masses forming igneous rocks bodies. Many studies have pointed out the relationship between the skarn-type minerals (as well as the composition of the causative igneous bodies), and the mineral deposits skarn-related [10,16]. It is very useful for mineral exploration to determine a cause-effect relationship between the causative igneous bodies and the skarn-type mineralogy, and establish the mineral chemistry of garnet and pyroxene, which is very important to postulate a specific type of skarn deposit according to the skarn-type mineralogy. The aim of this paper is to report the occurrence of the skarn-type mineralogy recognized in the Ciénaga Marbles. Based on the mineralogical characteristics observed in the skarn-type mineral assemblage, we also discuss its origin, which can be associated with the magmatic-hydrothermal event forming this skarn-type epigenetic mineral assemblage. Finally, based on previous regional geology studies and zircon U-Pb geochronology data, we report some considerations to propose a link between the Caribbean oceanic plate evolution and the magmatic hydrothermal system related to the skarn-type mineralogy formation.

2. Geological background

The study area belongs to the Santa Marta Massif (SMM), which constitutes an isolated triangular-shaped range on the northern Colombian Caribbean region and represents an uplifted region (with altitudes of ca. 5800 m), located along the diffuse southern Caribbean plate boundary (Fig. 1). This was the result of an oblique convergence between the Caribbean plate and northwestern South America [17-18]. The Oca fault [19], the Santa Marta-Bucaramanga fault [20], the Cerrejón thrust sheet [21] and the Romeral suture are the major structures bounding the SMM. It is composed mainly by crystalline rocks and can be divided into three belts (Sierra Nevada, Sevilla and Santa Marta), and has a defined outboard younging pattern from east to west. The southeastern and oldest Sierra Nevada belt includes ca. 1.0-1.2 Ga high grade metamorphic rocks represented by granulites, gneisses and amphibolites that were affected during the Grenvillian orogenic event [22-24]. Jurassic plutons and volcanites intrude and cover these metamorphic rocks. Minor Carboniferous and Late Mesozoic sedimentary sequences rest in unconformity towards the southeast [25-26]. The intermediate Seville belt represents a polymetamorphic complex that includes Paleozoic gneisses and schists with Permian millonitized peraluminous granitoids [25,27-28]. The northwestern and youngest Santa Marta belt comprises an inner sub-belt of Cretaceous imbricated metamorphic rocks (greenschists and amphibolites) and an outer sub-belt of Mesozoic amphibolites, greenschists and phyllites separated by the lower to middle Cenozoic Santa Marta Batholith (SMB) [26,29-30]. The Cesar-Rancheria basin, exposed in the southeastern flank of the SMM, represents a sedimentary record that evolved from a Cretaceous passive margin to Maastrichian-Paleogene orogenic deposits linked to an accretionay and subduction event of the Caribbean plate [31]. Several quarries exploiting the Ciénaga Marbles (Santa Marta Geotectonic Province) are situated to the east of Ciénaga (Magdalena) at 11°00' North, 74°15' West, which are easily accessible from Ciénaga. Access is via the Caribbean Transverse (National Route 90) that connects with the Magdalena Trunk (National Route 45), and then turning left and continuing for 0.35 km on an unpaved road.

Metamorphic rocks from the Gaira Schists and Ciénaga Marbles, and igneous rocks are grouped into the SMB and recent deposits occur in the study area (Fig. 2). The Ciénaga Marbles host a skarn-type mineralogy, which can be associated with a magnesian-type skarn, genetically related to granitic igneous activity from the Eocene age SMB. The Gaira Schists crop out towards the northwest of the SMB. They are the result of a Middle Eocene (58.4±4.3 Ma) regional low- to middle-grade metamorphism under the greenschist and amphibolite facies [24], which have undergone retrograde metamorphism and metasomatism with abundant dykes of pegmatite, aplite and dacite [24]. The Ciénaga Marbles (early Cretaceous in age) and its surroundings are part of the Santa Marta Geotectonic Province in the SMM - a polymetamorphic complex that includes gneisses and schists of Paleozoic age with Permian mylonitic granitoids [27]. In general, they are coarse-grained white and bright marbles with granoblastic texture and sutured contacts, although they can be fine-grained dark gray marbles with a banded structure. Their spatial distribution and geometry is not very well established and their stratigraphic relationships with the surrounding rocks are difficult to establish due to numerous faults surrounding the bodies.

The relationships between marbles and schists are uncertain and not determined in the field. The Ciénaga Marbles overlies the Gaira Schists (metamorphosed to amphibolite facies before the intrusion of the SMB). They are divided into two members: (1) relatively pure and low magnesium marbles and (2) impure, in part dolomitic, sandy marbles, calcareous metasediments, metamudstones and quartzites. The SMB [25] emerges as a NE trending belt located between metamorphic rocks and is composed of

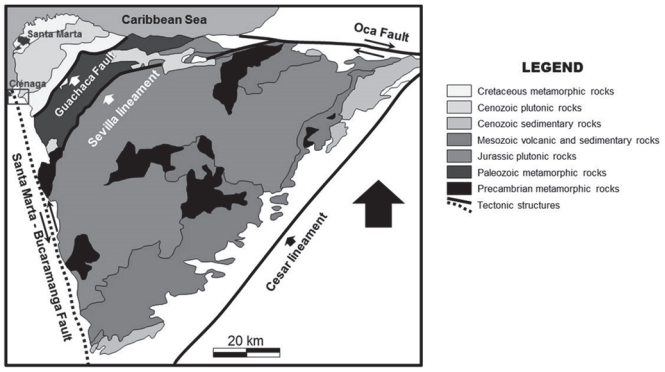

Figure 1. Generalized geological map of the SMM, showing the study area (small red line box).
Source: Adapted from Tschanz *et al*. [26].

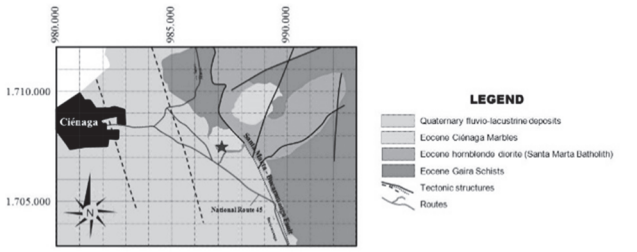

Figure 2. Geological map of the study area and distribution of the Ciénaga Marbles and sampling locality.
Source: Adapted after INGEOMINAS [34].

granodiorite to monzogranite with transitional variations and tonalite. It can show magmatic foliation similar to that reported by Gonzalez [35]. Mafic enclaves commonly occur throughout the body, with fewer pegmatitic hornblendites (cumulates of hornblende), indicating a complex magmatic history with recirculation and the mixing of materials from the lower parts of the magma chamber [36].

3. Field sampling and analytical methods

Marbles and associated rocks were collected from the mining area, taking into account their field relationships, texture and mineralogy. The petrographic analysis was performed on a trinocular NIKON LABOPHOT2-POL microscope. Mineral abbreviations are after Kretz [32]. SEM/EDS analysis was carried out by environmental scanning electron microscopy (FEI Quanta 650 FEG ESEM) under the following analytical conditions: magnification = 160-750x, HFW = 199 μm - 1.86 mm, HV = 20-30 kV, spot = 3.0, signal = SE, detector = LFD. Fractions of heavy mineral concentrates (<350 μm) were separated using traditional techniques at ZirChron LLC in Washington State University. LA-ICPMS U-Pb analyses were conducted at the GeoAnalytical Lab at the Department of Geology in Washington State University using a New Wave Nd:YAG UV 213-nm laser coupled to a ThermoFinnigan Element 2 single collector, double-focusing, and magnetic sector ICPMS. Operating procedures and parameters are discussed by Mantilla *et al*. [33].

4. Field relationships

White greyish, medium- to coarse-grained marbles of variable morphology (with sharp contacts) and thickness (from centimeter to meter scale) show a transition into carbonate-silicate rocks, which, in turn, pass into calc-silicate and carbonate-bearing silicate rocks. Finally, when carbonate tends to disappear, they are cut by porphyritic granodiorites (Fig. 3). They show a weak to strong banding (alternation of carbonate-rich and calc-silicate layers). Fig. 3a shows an excellent overview of the Bucaramanga - Santa Marta Fault. Fig. 3b shows a view of the El Futuro quarry; the actinolitic schist is at the top; and the marble is at the bottom. An intrusive contact zone between the actinolitic schist and the granodiorite is shown in Fig. 3c. Note the occurrence of part of the endoskarn (oxidation zones) and exoskarn (marble with reaction bands). Fig. 3d shows the occurrence of granodiorite with faneritic and

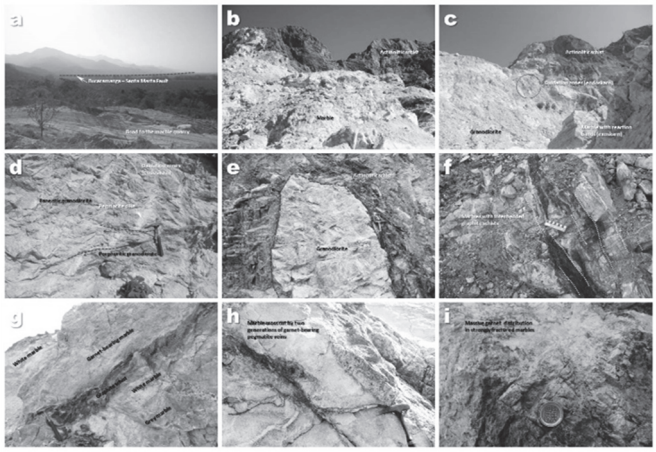

Figure 3. Field photographs of the Ciénaga Marbles and related rocks.
Source: The authors.

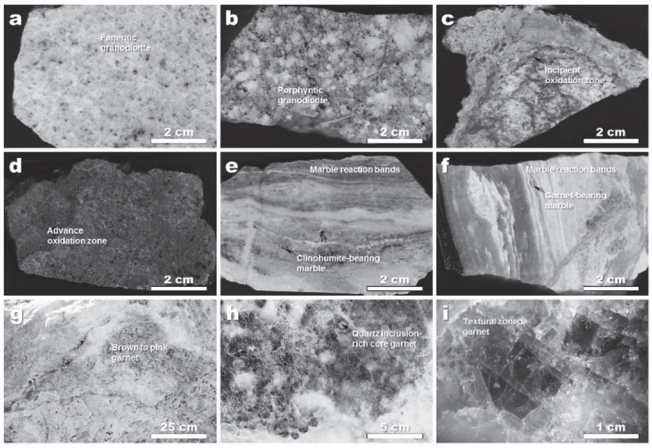

Figure 4. General macroscopic characteristics of the intrusive rocks (a)-(d) and Ciénaga Marbles (e)-(f). Photographs on several scales of the occurrence of brown to pink garnet aggregates in marble (g)-(i).
Source: The authors.

porphyritic textures, cross cut by a pegmatite, which have been affected by dextro-lateral faults; the oxidation zones (endoskarn) can be seen in the upper right part. Fig. 3e shows a well-defined intrusive contact between the granodiorite and the actinolitic schist. Note the characteristic tabular geometry of marbles interbedded with graphite schists in Fig. 3f. In Fig. 3g several marble types and interbedded graphite schists can be observed. Marble is commonly cross cut by two generations of garnet-bearing pegmatites (Fig. 3h). Fig. 3i shows the occurrence of massive brown to pink garnet in strongly fractured marbles.

General macroscopic characteristics of the Ciénaga Marbles and associated rocks are shown in Fig. 4. A granodiorite body cutting metamorphic rocks (actinolitic schists and marbles) shows a phaneritic and porphyritic texture (Figs. 4a-4b). In the endoskarn zone, incipient (Fig. 4c) to advanced (Fig. 4d) oxidation zones are developed. Figs. 4e-4f illustrates marble reaction bands. Massive brown to pink garnet aggregates commonly occur in marbles (Figs. 4g-4i).

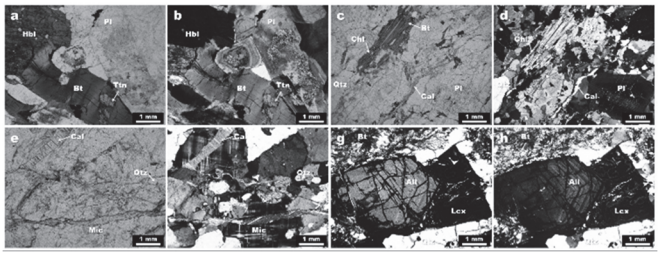

Figure 5. Endoskarn minerals in the intrusive rocks under the petrographic microscope.
Source: The authors.

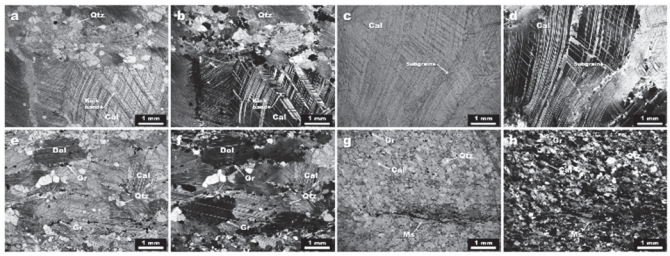

Figure 6. Petrographic features of the pure marble-forming minerals under the petrographic microscope.
Source: The authors.

5. Mineralogy and petrography

5.1. Causative rock

The emplacement of intrusive rocks belonging to the SMB (Fig. 5) affected marbles developed a skarn-type mineralogy. The main petrographic facies corresponds to a granodioritic intrusive (Figs 5a-5d), exhibits holocrystalline equigranular texture; and is mostly composed of plagioclase (well-developed albite twinning, characteristic sieve texture and alteration to sericite), quartz, biotite and hornblende, with minor zircon, titanite and apatite and chlorite as a retrograde phase. Locally, small garnet-bearing pegmatites cross cut the granodiorite (Fig. 5e-5f) and are mainly composed of quartz, plagioclase and microcline (tartan twinning), with minor epidote and muscovite, magnetite and zircon as accessory minerals, and chlorite and sericite as secondary minerals. Biotite represents a supergene mineral phase cross cut by calcite veinlets. The endoskarn zone presents a sulphide (pyrite) and oxidation (magnetite) zones, the latter with large crystals of allanite (typical textural oscillatory zoning and reaction rims of leucoxene, monacite and barite). Leucoxene can be cross cut by barite veinlets (Fig. 5g-5h). The original crystalline marbles were locally affected by a causative body (granodiorite), which gives rise to thin calc-silicate reaction bands with spotty garnet and diopside crystals near the boundary with the exoskarn zone.

5.2. Host rocks

5.2.1. Regional metamorphism (pre-skarn stage)

The regional metamorphic stage is represented by white, medium-grained, pure marbles that display a granoblastic fabric (Fig. 6). They are mostly composed of medium-grained recrystallized calcite and dolomite, and show characteristic rhombohedral cleavage and polysynthetic twinning. The associated minor minerals are quartz, muscovite and graphite. Very fine-grained zircon of high relief and extreme birrefringence occurs as inclusions in carbonates. The mineralogy of the pre-skarn stage is associated to regional metamorphism involving the recrystallization of calcite and dolomite to marbles.

5.2.2. Skarn stages

Impure marbles of the skarn stages are represented by carbonate rocks with a foliated structure and granoblastic texture. They are mainly composed by recrystallized magnesian calcite and dolomite as the dominant minerals, as well as a variety of minerals in the following petrographic classes: wollastonite-, forsterite-, diopside-, garnet-, clinohumite- and vesubianite-bearing marbles. Common minerals are graphite, quartz, diopside, garnet, wollastonite, clinohumite and forsterite. Minor minerals are tremolite, epidote-group minerals, clinochlore and muscovite. Accessory minerals are rutile, titanite, fluorapatite and pyrite. Secondary minerals are calcite and sepiolite.

Isochemical metamorphism involves recrystallization of sedimentary calcite and dolomite to coarse-grained impure marbles and changes in mineral stability without significant mass transfer. There is, thus, no injection or leaching out of new elements by magma or volatile fluids [3,37-38] involved. Previous studies of metamorphic phenomena emphasized the isochemical mineralogical changes due to metamorphic re-equilibration under differing PT regimes, although the metasomatic mass-transfer of chemical components is also recognized as an important process accompanying regional metamorphism [39-42]. Metamorphic recrystallization of carbonate and quartz and mineralogical changes affect the carbonate-bearing protolith, and circulating of high-T fluids promotes the formation of anhydrous calc-silicate minerals such as diopside, garnet (at ~400-700 °C), and probably titanite. Metasomatic metamorphism is a metamorphic process by which the chemical composition of a rock is altered in a pervasive manner and involves the introduction and/or removal of chemical components as a result of the interaction of the rock with aqueous fluids [43]. This is essentially a multistage metasomatism process, in which magma crystallizes and releases a fluid phase, producing a metasomatic skarn.

Prograde anhydrous stage. Garnet in the marble and barren skarn zones appear to show the anomalous anisotropy (which can be attributed to the presence of H_2O molecules in its chemical structure) more frequently than those in the mineralized skarn zone [44]. Fig. 7 shows the different textural morphologies of garnet under the petrographic microscope: garnet developing embayment (Figs. 7a-7b), disseminated aggregates of garnet (Figs. 7c-7d), highly tectonized garnet (Figs. 7e-7f), textural zoned garnet (Figs. 7g-7h), skeletal and idioblastic garnet (Figs. 7i-7j), garnet displaying a quartz rich inclusion-core and a poor-inclusion rim (Figs. 7k-7l).

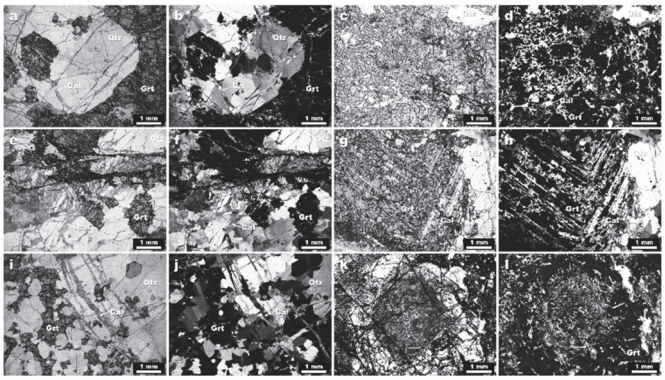
Figure 7. Skarn-type garnet of the prograde anhydrous stage displaying several textural morphologies.
Source: The authors.

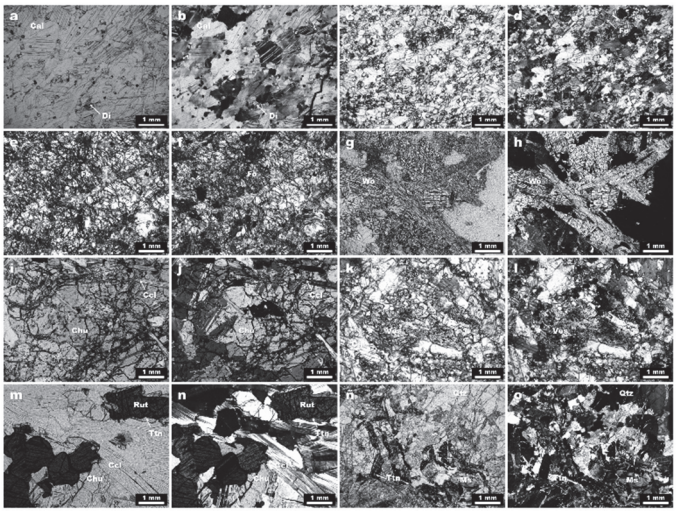
Figure 8. Skarn-type minerals of the prograde anhydrous stage.
Source: The authors.

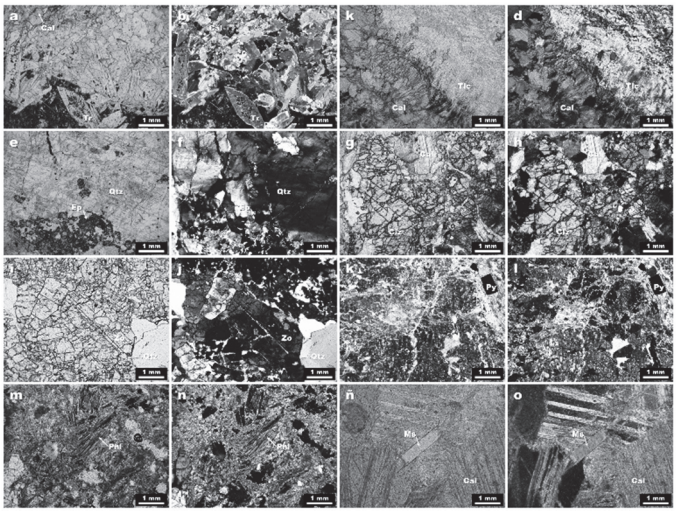
Figure 9. Skarn-type minerals from the prograde metasomatic stage.
Source: The authors.

The main petrographic aspects of the skarn-type minerals of this stage are shown in Fig. 8. Magnesian calcite occurs as very fine- to medium-grained recrystallized crystals of characteristic rhombohedral cleavage and polysynthetic twinning and is locally accompanied by dolomite. Diopside is the most abundant mineral occurring as a fine-grained granoblastic intergrowth with calcite. It has a typical short prismatic crystal or well-formed equant cross-sections, is clear to light green in color, has a high relief, near 90º cleavage angle, and interference colors that range (from blue to violet) up to mid second order (views that show two cleavages tend to be lower), and a large extinction angle. At the granodiorite-marble contact, a zone of diopside was observed. It could have been formed due to the diffusion of Ca, Mg and Si as suggested by Kenneth [45]. Occurrences of forsterite could represent the main mineral phase along with calcite and dolomite and minor phlogopite. Forsterite is largely replaced by serpentine (typical mesh texture) and comprises rounded crystals of up to 4.5 mm in size that are cut by serpentine veins. Alternating poor-wollastonite and rich-wollastonite zones can be recognized. Wollastonite is formed by the infiltration of H_2O-rich fluids close to the peak of regional metamorphism, although it can also be formed by the calcite + quartz = wollastonite + CO_2 [46] reaction. Clinohumite shows typical pleochroism from pale yellow to red-yellow and is locally intergrown with forsterite. Vesubianite occurs as scarce pleochroic (yellow to orange) crystals dispersed in the matrix. Rutile is spatially associated with dolomite marble and occurs as large grains or aggregates mimicking the occurrence of Fe-Ti oxides in the protolith. Titanite occurs in the matrix as very fine-grained aggregates with the characteristic brown color and high relief. It is in contact with calcite and diopside. Fluorapatite occurs as scattered small grains.

Prograde metasomatic stage. Fig. 9 shows the main minerals in this stage. Tremolite occurs as colorless crystals of high relief and third order interference colors, which are in contact with calcite. Very fine-grained epidote shows the typical slight pleochroism. It occurs as inclusions in calcite. Clinozoisite is colorless and shows high relief and fractures filled by quartz and calcite. Zoisite occurs as fine-grained, colorless and very high relief crystals that shows anomalous interference colors. Platy bronze brown to pale orange phlogopite shows weak pleochroism, perfect cleavage on (001) and straight extinction. Muscovite occurs as individuals of straight and serrated boundaries.

Retrograde meteoric stage. It is structurally controlled and overprints the prograde zonation sequence such as garnet and diopside. The retrograde skarn-type minerals can show vein structure. Fig. 10 shows the main minerals of the retrograde meteoric stage, which is represented by the occurrence of calcite, quartz, chlorite, serpentine, sepiolite and pyrite. Veins of quartz-calcite, which are cutting massive garnet, can be related to retrograde skarnization. In the later stage of alteration, chlorite occurs as fibrous aggregates locally replacing phlogopite. Abundant quartz occurs as fine-grained inclusions in garnet or as a matrix constituent. Coarse-grained quartz associated to skeletal garnet is cut by calcite veinlets. It sometimes occurs in complex veins, showing elongated aggregates growing over a carbonate matrix with bubbles extensions that penetrate veinlets of fibrous sepiolite aggregates. Serpentine occurs after forsterite, which implies that H_2O must have remained the dominant fluid during retrograde calc-silicate formation [47],

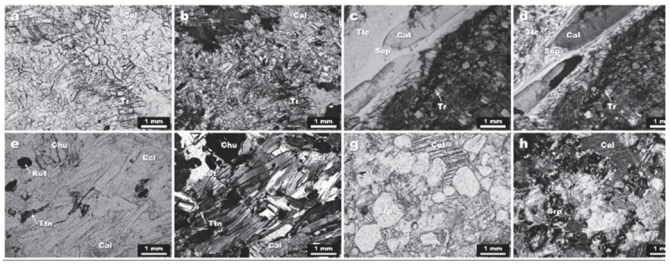

Figure 10.Retrograde minerals under the petrographic microscope.
Source: The authors.

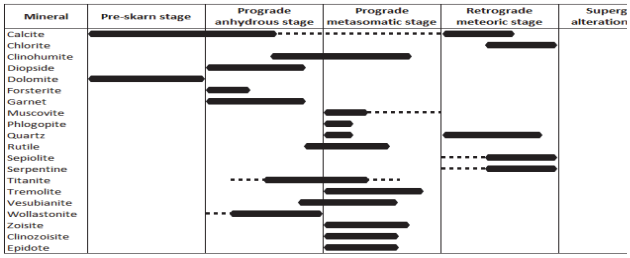

Figure 11. Paragenetic sequence of exoskarn and ore minerals from the Ciénaga Marbles.
Source: The authors.

and must be related to a low-T hydrothermal/metasomatic process [48]. It also can be formed after replacement of clinohumite and diopside. Pyrite occurs as small crystals with edges showing a bronze color and is related to calcite veinlets.

5.2.3. Supergene alteration stage

This stage is represented in the endoskarn zone and is characterized by the local occurrence of pyrite and magnetite. Moreover, in the oxidation zone, large crystals of textural zoned allanite display a strong replacement by leucoxene, although, they is also rimmed by monacite and leucoxene. Barite, occurring as a precipitated phase, rims allanite or develops veinlets cross cutting leucoxene.

Petrographic analysis of the Ciénaga Marbles, located in proximity to granitic dikes and stocks of the SMB, reveals the paragenetic sequence described above, which is shown in Fig. 11. The inexistence of ore skarn can be associated to erosion.

6. Mineral chemistry

Fig.12 shows the textural relationships observed in the skarn minerals. Figs. 12a-12c illustrate mineral relationships in the endoskarn zone. Fig. 12a shows a large garnet cross cut by quartz microveins. Fig. 12b shows a subhedral magnetite in a matrix mainly composed of quartz and chlorite with minor calcite and titanite and fluorapatite as the main accessory minerals. A large subhedral magnetite rimmed and cross cut by barite microveins can be observed in Fig. 12c. The association magnesian calcite + dolomite + clinohumite + forsterite (replaced by serpentine) is shown in Fig. 12d. Fig. 12e shows the occurrence of clinohumite along with dolomite + magnesian calcite. A replacement of forsterite by serpentine is observed in Fig. 12f; the presence of clinohumite, dolomite, magnesian calcite and clinochlore can also be noted. Fig. 12g shows fluorapatite along with magnesian calcite and clinochlore; numerous veins of magnesian calcite cross cut fluorapatite. The wollastonite + diopside + calcite association is shown in Fig. 12h. Fig. 12i shows abundant dolomite and scarce magnesian calcite that occur as matrix phases or as secondary veins cross cutting dolomite.

The retrograde stage can be documented by the occurrence of fibrous sepiolite and veinlets of barite. Similar fibrous clays have been reported by Zaaboub *et al*. [49]. According to the previous sepiolite would have precipitated directly in hydrothermal environments under alkaline conditions, high Si and Mg and low Al activity. Veinlets of barite (barium sulfate) reveals that the presence of other minerals in the precursor hydrothermal solution affected the kinetics of crystal growth of barium sulphate as has beeb reported in several studies [50-51]. In general, magnesian skarns form at temperatures 450-750 ºC and pressures of 0.5-10 kbar, they contain forsterite, diopside, clinohumite and phlogopite at the contacts between magmatic and calc-magnesian or magnesian carbonate rocks, typically host ores, and may develop in both the magmatic (prograde, in contact with magmatic fluids) and postmagmatic (retrograde) stages [42]. We suggest that the magnesian skarn-type mineralogy hosted in the Ciénaga Marbles is related to the magmatic stage of the SMB and is characterized by the occurrence of magnesian calcite and/or dolomite, forsterite and pyroxene, with the last of these occurring only due to low chemical activity of CaO. However, it can be also related to the postmagmatic stage of the SMB. A very complex skarn-type mineralogy zonation can be observed. According to Pertsev [52], magnesian skarns of both stages are commonly replaced in varying degrees by postmagmatic calc-skarns under moderate P-T conditions due to increasing CaO chemical

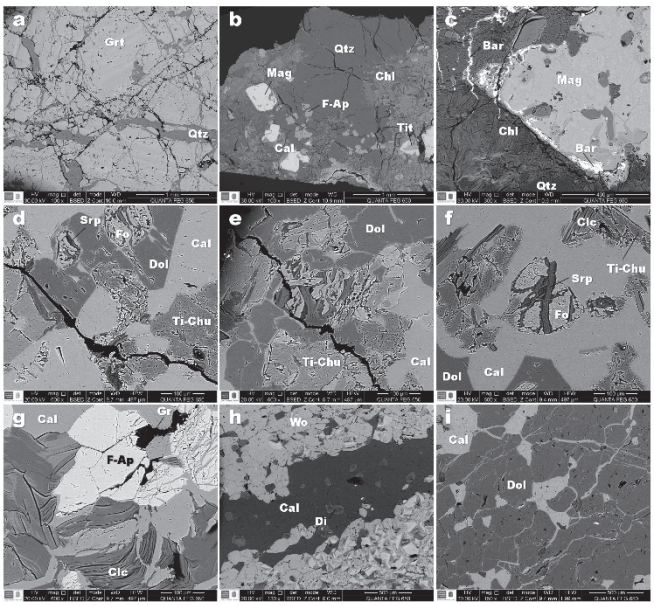

Figure 12. SEM photomicrographs of the textural relationships between skarn-type minerals.
Source: The authors.

activity with decreasing temperature and a corresponding decrease of CO_2 concentration in fluids. Therefore, low-T post-skarn alteration leads to the replacement of skarn minerals by serpentine and carbonates. Ore mineralisations accompanying the formation of magnesian skarns are magnetite and borates (ludwigite, suanite and kotoite), with a wide variety of ore mineralizations (e.g., Cu, Mo, W, Be, Sn, Pb, Zn, Au, B) that can be overprinted by low-T hydrothermal processes [42]. This the case reported in this study.

7. Skarn and ore minerals

Skarns are defined by their mineralogy, which includes a wide variety of calcium-bearing silicates and associated minerals, but is usually dominated by garnet and pyroxene [3]. Skarns can be subdivided according to several criteria. However, skarns are broken down into two broad subcategories [3,53]: exoskarns and endoskarns. In the study area, the skarn is divided into exoskarn, with subordinate endoskarn (centimeter-wide altered plutonic rocks in contact with the skarn) and skarn veins. An exoskarn can be recognized in the marbles close to the thermal source (magma or hydrothermal fluids). An endoskarn developed within the granodiorite intrusion is represented by highly sulphidation (pyrite) and oxidation (magnetite) zones, the last of these has the appearance of zoned allanite, which is rimed by monacite and cross cut by barite. Skarns may or may not host economic reserves of metals. If they do they are called skarn deposits, which are often described according to the dominant economic metal or mineral present, whether it is Cu, Fe, W, Zn-Pb, Mo, Au, etc. However, the majority of the world's economic skarn deposits occur in calcic exoskarns. The Ciénaga skarn is a magnesian type, which can explain why there is no ore zone. It can be considered as a reaction of magnesian skarn that is formed by isochemical metamorphism of thinly interlayered shales and limestones where the metasomatic transfer of components between adjacent lithologies may occur on a small scale, as suggested by some authors [2]. The previously mentioned lithological and mineralogical features (magnesian skarn-type mineralogy) may suggest a potential environment for the formation for Fe, Sn (W), Be, B, and REE deposits.

8. Skarn-type mineralogy zonation in the Ciénaga Marbles

Most skarns show a general zonation pattern of proximal garnet, distal pyroxene and vesubianite at the contact between skarn and marble. Skarn minerals may display systematic color or compositional variations within the larger zonation pattern [42]. Atkinson and Einaudi [4] describe it, with proximal garnet being commonly dark red-brown, becoming lighter brown and finally pale yellow-green near the marble front. A granodiorite of the SMB intruded into the Ciénaga Marbles. Metamorphism and metasomatism produced millimeter to centimeter scale reaction zones near the contact. The contact zone shows evidence of assimilation of the marbles by granodioritic magma. Most major skarn deposits are directly related to igneous activity and broad

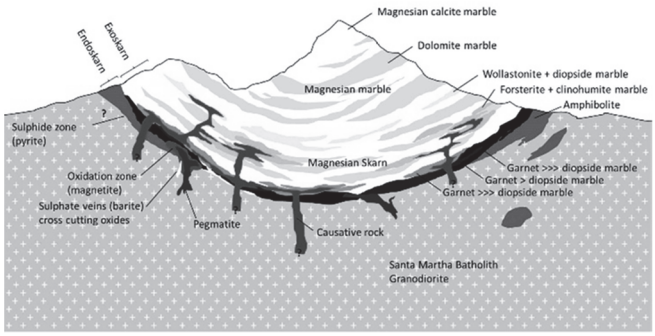

Figure 13. Idealized cross section (not to scale) through the skarn-type mineral distribution in the Ciénaga Marbles.
Source: The authors.

correlations between igneous composition and skarn type have been previously described [1,5]. We suggest a zonation pattern for the skarn-type mineralogy, which does not extend on a large area, although it can provide important evidence as exploration guides. We suggest that skarn-type minerals were formed at different stages and P-T conditions, not coexisting each other based on the general idea of chemical equilibrium. Fig. 13 shows an idealized cross section through the skarn-type mineral distribution in the Ciénaga Marbles. The following zones and mineral assemblages were identified (in order of decreasing grade): The endoskarn is developed within the granodiorite intrusion and is represented by very small sulphidation (pyrite) and oxidation (magnetite) zones; the last of them with the occurrence of zoned allanite, rimed by monacite and leucoxene and cross cutting by barite veinlets. The exoskarn is represented by the following zones: Garnet zone (next to the contact) consists of grossularite garnet, diopside, and minor calcite and quartz. We have no evidence on the occurrence of pale green garnet, then, we suggest that a proximal red-brown to brown garnet can be close to the marble. The change in pyroxene color is less pronounced but typically reflects a progressive increase in Fe and/or Mn towards the marble front [54], which has not been confirmed yet in the study area. Diopside zone mainly composed of diopside and calcite, and minor garnet. Monticellite zone contains magnesian calcite, dolomite, clinohumite, forsterite, phlogopite, with serpentine as the main retrograde mineral phase. Taking into account that these minerals are absent in most other types of skarn [42], this reveals a magnesian skarn-type mineralogy. Idocrase (vesubianite) zone consists of vesubianite in association with calcite, diopside, wollastonite and phlogopite. Inner zone consists of magnesian calcite and dolomite marble, showing little metasomatism.

9. U-Pb Geochronology

Sample SMS-2-3 (granodiorite cutting the Cienaga Marbles) was dated by U/Pb (Table 1). It was collected and dated due to its close relationship to the skarn-type mineralogy developed around its borders. Analytical data and U-Pb isotope ratios indicate the presence of at least two ages: the first one is made up of 27 of the 42 performed analysis

(~64% of all analyzes, with ages ranging from 60.7 to 54.3±0.7 Ma; and the second one is made up of 15 of the 42 performed analysis (~ 36% of all analyzes), with ages ranging from 1065.3±15 to 62.8±0.8 Ma. After considering the analytical and systematic error (Fig. 14), the first group of ages can be clearly related to the crystallization of a granitoid at 55.5±0.7 Ma. Taking into account that the skarn-type mineralogy is the result of magmatic-hydrothermal processes and is developed around granitic rocks, we suggest that the formation of the skarn-type mineralogy occurred at the same time as the granitoid crystallized. This absolute age coincides with when the onset of magmatism developed: the start of the change in polarity of the subduction of the Caribbean plate beneath of the South American plate. This is in accordance with the model proposed by Cardona *et al*. [27], and is part of a more regional scale model proposed by others [55-56]. Similar ages for this magmatism were reported by Mejía *et al*. [28]. We assume these magmas correspond to molten silicate enriched in hydrothermal fluids and, therefore, they should be considered to be of high interest for mineral exploration due to their ability to form magmatic-hydrothermal systems. The second group of ages led to the following subgroups being differentiated: (1) with 3 ages ranging from 62.8±0.8 to 79.9±1.3 Ma, (2) with 6 ages ranging from 98.6±1.4 to 143.4±1.7 Ma, (3) with 2 ages ranging from 230.3±3.3 to 235.1±3.1 Ma, (4) with 1 age of 444.8±5.0 Ma, and (5) with 2 ages ranging from 1057.8±15.3 to 1065.3±15 Ma. The SMS-2-3-14 analysis (244.9±3.2 Ma) is excluded from the above groups because it is projected to some distance from the concordia curve (Fig. 14a). It is possible to suggest that the ages ranging from 62.8±0.8 to 79.9±1.3 Ma (Late Cretaceous - Early Paleocene) may be legacies that represent mainly derived zircons of oldest igneous rocks, such as those reported by Cardona *et al*. [27]. They can also be been formed in tectonic environments of intra-oceanic magmatic arcs and in environments own of a late collisional stage.

Table 1.
U–Pb analytical results in different zones within the zircons studied in SMS-2-3 sample that correspond to ages measured by LA-ICPMS.

Points of analysis	U ppm	Th U	$^{238}U/^{206}Pb$	1 σ (%-e)	$^{207}Pb/^{206}Pb$	1 σ (%-e)	$^{206}Pb/^{238}U$ age (Ma)	1 σ (abs-e)	$^{207}Pb/^{206}Pb$ age (Ma)	1 σ (abs-e)	Best age (Ma)	1 σ (abs-e) (Ma)
SMS-2-3_42	2.188	0.27	1.144.541	1.39	0.0469	1.17	56.1	0.8	43.0	27.9	**56.1**	**0.8**
SMS-2-3_41	825	0.35	1.156.547	1.44	0.0473	1.54	55.5	0.8	65.2	36.2	**55.5**	**0.8**
SMS-2-3_40	1.060	0.41	1.080.091	1.46	0.0475	1.58	59.4	0.9	74.4	37.1	**59.4**	**0.9**
SMS-2-3_39	845	0.31	1.173.206	1.45	0.0528	1.60	54.7	0.8	321.5	36.0	**54.7**	**0.8**
SMS-2-3_38	2.666	0.11	562.595	1.39	0.0490	0.78	113.6	1.6	147.2	18.1	**113.6**	**1.6**
SMS-2-3_37	1.080	0.31	1.153.490	1.78	0.0484	2.53	55.6	1.0	119.0	58.6	**55.6**	**1.0**
SMS-2-3_36	1.554	0.26	1.174.055	1.47	0.0487	1.29	54.7	0.8	135.0	29.9	**54.7**	**0.8**
SMS-2-3_35	645	0.31	1.162.160	1.56	0.0482	2.01	55.2	0.9	108.3	46.8	**55.2**	**0.9**
SMS-2-3_34	309	0.31	445.445	1.60	0.0518	1.92	143.1	2.3	277.8	43.3	**143.1**	**2.3**
SMS-2-3_33	1.163	0.38	1.130.086	1.45	0.0480	1.53	56.8	0.8	99.1	35.8	**56.8**	**0.8**
SMS-2-3_32	1.026	0.24	1.113.687	1.42	0.0464	1.62	57.6	0.8	17.9	38.4	**57.6**	**0.8**
SMS-2-3_31	506	0.24	1.151.824	1.66	0.0473	2.74	55.7	0.9	65.7	64.0	**55.7**	**0.9**
SMS-2-3_30	1.133	0.22	1.163.056	2.26	0.0478	2.47	55.2	1.2	90.2	57.4	**55.2**	**1.2**
SMS-2-3_29	949	0.33	1.183.233	1.31	0.0475	1.63	54.3	0.7	75.4	38.3	**54.3**	**0.7**
SMS-2-3_28	932	0.40	833.424	1.76	0.0494	1.47	76.9	1.3	164.8	34.1	**76.9**	**1.3**
SMS-2-3_27	1.157	0.48	1.181.463	1.29	0.0471	1.57	54.3	0.7	55.5	37.1	**54.3**	**0.7**
SMS-2-3_26	1.759	0.03	1.021.716	1.23	0.0476	1.20	62.8	0.8	81.4	28.3	**62.8**	**0.8**
SMS-2-3_25	2.089	0.58	139.991	1.17	0.0562	0.65	444.8	5.0	461.9	14.4	**444.8**	**5.0**
SMS-2-3_24	1.194	0.34	1.175.772	1.45	0.0464	1.97	54.6	0.8	19.6	46.7	**54.6**	**0.8**
SMS-2-3_23	519	0.31	77.217	1.17	0.0749	0.75	785.0	8.7	1065.3	15.0	**1065.3**	**15.0**
SMS-2-3_22	1.224	0.51	1.163.784	1.31	0.0470	1.43	55.2	0.7	47.0	33.9	**55.2**	**0.7**
SMS-2-3_21	993	0.30	1.153.031	1.25	0.0469	1.73	55.7	0.7	46.6	40.9	**55.7**	**0.7**
SMS-2-3_20	1.652	0.33	444.559	1.19	0.0488	0.95	143.4	1.7	137.8	22.2	**143.4**	**1.7**
SMS-2-3_19	1.015	0.46	1.154.251	1.41	0.0493	1.42	55.6	0.8	160.9	32.8	**55.6**	**0.8**
SMS-2-3_18	704	0.30	1.156.202	1.48	0.0472	1.87	55.5	0.8	59.2	43.9	**55.5**	**0.8**
SMS-2-3_17	837	0.34	1.159.776	1.42	0.0488	1.47	55.3	0.8	138.5	34.1	**55.3**	**0.8**
SMS-2-3_16	760	0.34	1.156.884	1.39	0.0482	1.53	55.5	0.8	109.0	35.7	**55.5**	**0.8**
SMS-2-3_15	881	0.34	1.216.329	1.89	0.0489	2.92	52.8	1.0	144.4	67.1	**52.8**	**1.0**
SMS-2-3_14	629	0.20	258.285	1.32	0.0545	0.76	244.9	3.2	392.8	16.9	**244.9**	**3.2**
SMS-2-3_13	1.134	0.14	552.158	1.49	0.0492	1.00	115.7	1.7	158.6	23.2	**115.7**	**1.7**
SMS-2-3_12	614	0.68	649.008	1.44	0.0481	1.28	98.6	1.4	104.8	30.0	**98.6**	**1.4**
SMS-2-3_11	1.859	0.16	1.127.777	1.39	0.0473	1.36	56.9	0.8	63.1	32.0	**56.9**	**0.8**
SMS-2-3_10	638	0.15	1.152.014	2.75	0.0516	1.76	55.7	1.5	265.6	39.8	**55.7**	**1.5**
SMS-2-3_9	2.168	0.31	500.368	1.62	0.0490	0.63	127.6	2.0	145.9	14.7	**127.6**	**2.0**
SMS-2-3_8	899	0.36	1.163.266	1.43	0.0472	1.33	55.2	0.8	57.7	31.5	**55.2**	**0.8**
SMS-2-3_7	306	0.64	274.890	1.44	0.0529	1.31	230.3	3.3	323.6	29.5	**230.3**	**3.3**
SMS-2-3_6	1.165	0.56	1.057.737	1.63	0.0494	1.35	60.7	1.0	169.0	31.3	**60.7**	**1.0**
SMS-2-3_5	521	0.27	269.250	1.36	0.0509	1.11	235.1	3.1	235.9	25.5	**235.1**	**3.1**
SMS-2-3_4	720	0.34	1.157.765	1.53	0.0478	1.70	55.4	0.8	89.1	39.9	**55.4**	**0.8**
SMS-2-3_3	542	0.14	65.228	1.35	0.0746	0.77	919.5	11.6	1057.8	15.3	**1057.8**	**15.3**
SMS-2-3_2	809	0.57	867.787	1.55	0.0490	1.20	73.9	1.1	148.8	28.0	**73.9**	**1.1**
SMS-2-3_1	971	0.13	1.138.402	1.45	0.0483	1.45	56.4	0.8	112.7	33.8	**56.4**	**0.8**

Source: The authors.

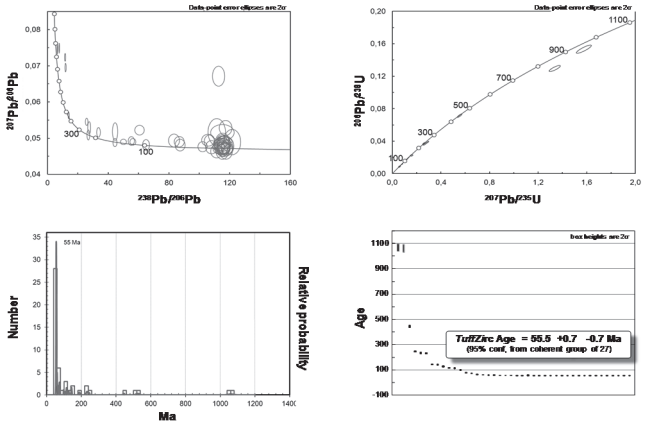

Figure 14. U-Pb ages obtained from zircon analyses in sample SMS-2-3. (a)-(b) U-Pb concordia diagrams, showing inheritance and crystallization ages of the granitic body. (c) Diagram of distribution of age ranges, showing the dominance of ages around 55 Ma. (d) Distribution diagram of all ages (error 2s).
Source: The authors.

The latter is considered to be the cause of the terminal magmatism, developed prior to the change in polarity of subduction. We also consider that some of these values represent mixed ages obtained at intermediate possible areas zoned zircons. Therefore, ages ranging from 98.6±1.4 to 143.4±1.7 Ma should be considered. However, considering that they represent older magmatic events (mainly Early Cretaceous), and not a mix of ages, these data could be very important as they may be indicating older magmatic events probably related to the geological evolution of the Caribbean's earliest stages. Ages between 230.3±3.3 and 235.1±3.1 Ma (Triassic) may be related to inherited zircons from rocks associated to the Triassic-Jurassic magmatic period documented in several studies [22,24-27,30,58]. They may also represent a mix of ages obtained at intermediate areas of zoned zircons. The age of 444.8±5.0 Ma (Ordovician Late) may be related to inherited zircons from rocks associated with the Paleozoic Early magmatic period [58]. Ages from 1057.8±15.3 to 1065.3±15 Ma can be attributed to inherited zircons from Grevillian metamorphic rocks reported in the Northern Andes, particularly in the SMM.

10. Conclusions

The Ciénaga Marbles that formed in a magmatic arc tectonic environment (emplacement of the lower to middle Cenozoic SMB), developed in a continental crust. The skarn-type mineralogy is hosted in lower Cretaceous marbles, and it is related to small granitic dikes and stocks. The Ciénaga skarn-type mineralogy is regarded to have formed by the reactions of the lower Cretaceous carbonate sedimentary sequence with the SMB, although it cannot be considered as a skarn deposit. The main general features of the skarn-type mineralogy are summarized as follows: (1) A typical exoskarn with a magnesian skarn-type mineralogy can be recognized; however, we cannot rule the existence of a calcium skarn-type mineralogy. (2) The exoskarn is composed mainly of garnet and diopside. (3) A late stage is composed of hydrous minerals such as sepiolite, chlorite and serpentine. (4) The occurrence of clinohumite confirms the occurrence of a magnesian skarn-type mineralogy at the Ciénaga Marbles. The presence of clinohumite, serpentine and Mg-chlorite would represent minerals of the retrograde stage. We also consider that the presence of forsterite, pyroxene and garnet belong to the prograde or isochemical metamorphism stage. (5) A skarn-type mineralogy was recognized and its precursor mineralogy is mainly represented by dolomitic marbles to explain the development of a magnesian skarn. (6) Taking into account that this term should be applied to a mixture of calcic and magnesian marbles, we suggest that this is not a calcic-magnesian system. (7) The obtained zircon U-Pb ages (from granodioritic bodies) yielded an age of 55.5±0.7 Ma (Ypresian, Early Eocene), which is also assumed to be the age of the formation of the skarn-type mineralogy in the Ciénaga Marbles and coincides with the beginning of the subduction polarity change (*i.e.* when the Caribbean oceanic plate began to subduct beneath South American continental plate).

Acknowledgments

We are grateful to geologist H. Cotes for the support on our visits to the marble quarry. Thanks to the Universidad Industrial de Santander and Universidad de Pamplona for providing us research facilities. Thanks to the Microscopy Laboratory in the Guatiguará Technological Park and its professional staff for assistance with SEM data acquisition. The manuscript was greatly improved based on the critical and helpful reviews and comments by anonymous reviewers. We are most grateful to the previously mentioned people and institutions for their support.

References

[1] Zharikov, V.A., Skarns. International Geology Review, 12(5-6), pp. 541-559, pp. 619-647, 1970. DOI: 10.1080/00206817009475262.

[2] Zarayskiy, G.P., Zharikov, V.A., Stoyanovskaya, F.M. and Balashov, V.N., The experimental study of bimetasomatic skarn formation. International Geology Review, 29(6), pp. 761-858, 1987. DOI: 10.1080/00206818709466181.

[3] Meinert, L.D., Dipple, G.M. and Nicolescue, S., World skarn deposits. In: Hedenquist. J.W., Thompson. J.F.H., Goldfarb. R.J., Richards. J.P., Editors, Economic Geology 100th Anniversary Volume, Society of Economic Geologists, Inc. Littleton, Colorado pp. 299-336, 2005. DOI: 10.2113/gsecongeo.77.4.745.

[4] Atkinson, W.W.,Jr. and Einaudi, M.T., Skarn formation and mineralization in the Contact Aureole at Carr Fork, Bingham, Utah. Economic Geology, 73(7), pp. 1326-1365, 1978. DOI: 10.2113/gsecongeo.73.7.1326.

[5] Einaudi, M.T., Meinert, L.D. and Newberry, R.J., Skarn deposits. Economic Geology, 75, pp. 317-391, 1981.

[6] Newberry, R.J. and Einaudi, M.T,. Tectonic and geochemical setting of tungsten skarn mineralization in the Cordillera. Arizona Geological Society Digest, 14, pp. 99-112, 1981.

[7] Einaudi, M.T. and Burt, D.M., Introduction - terminology, classification, and composition of skarn deposits. Economic Geology, 77, pp. 745-754, 1982. DOI: 10.2113/gsecongeo.77.4.745

[8] Burt, D.M., Skarn deposits - Historical bibliography through 1970. Economic Geology, 77, pp. 755-763, 1982. DOI: 10.2113/gsecongeo.77.4.745.

[9] Meinert, L.D., Gold skarn deposits - Geology and exploration criteria. Economic Geology, 6, pp. 537-552, 1989. DOI: 10.2113/gsecongeo.101.1.199.

[10] Meinert, L.D., Skarns and skarn deposits. Geoscience Canada, 19, pp. 145-162, 1992. DOI: 10.2113/gsecongeo.95.6.1183.

[11] Meinert, L.D., Compositional variation of igneous rocks associated with skarn deposits - Chemical evidence for a genetic connection between petrogenesis and mineralization: In Thompson, J.F.H., Eds., Magmas, fluids, and ore deposits, Mineralogical Association of Canada Short Course Series, 23, pp. 401-418, 1995. DOI: 10.1016/j.oregeorev.2015.08.004.

[12] Meinert, L.D., Application of skarn deposit zonation models to mineral exploration. Exploration and Mining Geology, 6, pp. 185-208, 1997.

[13] Meinert, L.D., A review of skarns that contain gold. Mineralized Intrusion - Related Skarn systems: Mineralogical Association of Canada Short Course, 26, pp. 359-414, 1998.

[14] Newberry, R.J., W. and Sn-Skarn deposits: A 1998 Status Report. Mineralized Intrusion - Related Skarn Systems: Mineralogical Association of Canada Short Course, 26, pp. 289-335, 1998.

[15] Meinert, L.D., Lentz, D.R. and Newberry, R.J., Introduction to a Special Issue Devoted to Skarn Deposits. Economic Geology, 95, pp. 1183-1184, 2000. DOI: 10.2113/95.6.1183.

[16] Swanson, S.E., Newberry, R.J., Coulter, G.A. and Dyehouse, T.M., Mineralogical variation as a guide to the petrogenesis of the tin granites and related skarns, Seward Peninsula, Alaska. Geological Society of America Special Paper, 246, pp. 143-160, 1990. DOI: 10.1130/SPE246-p143.

[17] Pindell, J.L., Higgs, R. and Dewey, J.F., Cenozoic palinspastic reconstruction, paleogeographic evolution and hydrocarbon setting of the northern margin of South America. In: Pindell, J.L. and Drake, C.L., Eds., Paleogeographic evolution and non-glacial eustasy, northern South America. Society of Economic and Petroleum Mineralogists Special Publication, 58, pp. 45-85, 1998.

[18] Moreno-Sánchez, M. and Pardo-Trujillo, A., Stratigraphical and sedimentological constraints on western Colombia: Implications on the evolution of the Caribbean plate. In: Bartolini, C., Buffler, R.T., Blickwede, J., Eds., The Circum-Gulf of Mexico and the Caribbean: Hydro-carbon habitats, basin formation and plate tectonics. AAPG Memoir, 79, pp. 891-892, 2003.

[19] Irving, E.M., Structural evolution of the northernmost Andes, Colombia. USGS Professional Paper 846, Washington DC, 27 P., 1971. DOI: 10.1017/S0016756800050780.

[20] Campbell, C.J., The Santa Marta wrench fault of Colombia and its regional setting. In: Saunders, J.B., Ed., Transactions of the Fourth Caribbean Geological Conference. Port-of-Spain, pp. 247-262, 1965.

[21] Kellogg, J., Cenozoic and tectonic history of the Sierra de Perijá, Venezuela-Colombia, and adjacent basins. GSA Memoir, 162, pp. 239-261, 1984. DOI: 10.1130/MEM162-p239.

[22] Restrepo-Pace, P.A., Ruiz, J., Gehrels, G. and Cosca, M., Geochronology and Nd isotopic data of Grenville-age rocks in the Colombian Andes: New constraints for late Proterozoic – early Paleozoic paleocontinental reconstructions of the Americas. Earth and Planetary Science Letters, 150, pp. 427-441, 1997. DOI: 10.1016/S0012-821X(97)00091-5.

[23] Ordóñez-Cardona, O., Pimentel, M.M. y De Moraes, R., Granulitas de Los Mangos: Un fragmento grenviliano en la parte SE de la Sierra Nevada de Santa Marta. Revista Academia Colombina de Ciencias, 26, pp. 169-179, 2002.

[24] Cordani, U., Cardona, A., Jiménez, D., Liu, D. and Nutman, A., Geochronology of Proterozoic basement inliers in Colombian Andes: Tectonic history of remnants of a fragmented Greenville belt. In: Vaughan, A., Leat, P., Pankhurst, R., Eds., Terrane processes at margins of Gondwana. Geological Society, London, Special Publications, 246, pp. 329-346, 2005.

[25] Tschanz, C.M., Marvin, R.F. and Cruz, B., Geology of the Sierra Nevada de Santa Marta (Colombia) - Informe 1829. INGEOMINAS, Bogotá, 1969.

[26] Tschanz, C., Marvin, R., Cruz, J., Mehnert, H. and Cebula, E., Geologic evolution of the Sierra Nevada de Santa Marta. Geological Society of America Bulletin, 85, pp. 269-276, 1974. DOI: 10.1130/0016-7606(1974)85<273:GEOTSN>2.0.CO;2.

[27] Cardona, A., Valencia, V., Bustamante, C., García-Casco, A., Ojeda, G., Ruiz, J., Saldarriaga, M. and Weber, M., Tectono-magmatic setting and provenance of the Santa Marta Schists, northern Colombia: Insights on the growth and approach of Cretaceous Caribbean oceanic terranes to the South American continent. Journal of South American Earth Sciences, 29, pp. 784-804, 2010. DOI: 10.1016/j.jsames.2009.08.012.

[28] Mejía, H.P., Santa, E.M., Ordóñez-Cardona, O. y Pimentel, M., Consideraciones petrográficas, geoquímicas y geocronológícas de la parte occidental del batolito de Santa Marta. DYNA, 75(155), pp. 223-236, 2008.

[29] Doolan, B.L., The structure and metamorphism of the Santa Marta area Colombia, South America. PhD Thesis, New York State University, New York, USA 1970, 200 P.

[30] MacDonald, W.D., Doolan, B.L. and Cordani, U.G. Cretaceous – Early Tertiary metamorphic K–Ar age values from the South Caribbean. Geological Society of America Bulletin, 82, pp. 1381-1388, 1971. DOI: 10.1130/0016-7606(1971)82[1381:CTMKAV]2.0.CO;2.

[31] Bayona, G., Lamus-Ochoa, F., Cardona, A., Jaramillo, C., Montes, C. y Tchegliakova, N., Procesos orogénicos del Paleoceno para la Cuenca Ranchería (Guajira, Colombia) y áreas adyacentes definidos por análisis de procedencia. Geología Colombiana, 32, pp. 21-46, 2007.

[32] Kretz, R., Symbols for rock-forming minerals. American Mineralogist, 68, pp. 277-279, 1983. DOI: 10.2138/am.2010.3371.

[33] Mantilla-Figueroa, L.C., Bissig, T., Valencia, V. and Craig, H., The magmatic history of the Vetas-California mining district, Santander Massif, Eastern Cordillera, Colombia. Journal of South American Earth Sciences, 45, pp. 235-249, 2013. DOI: 10.1016/j.jsames.2013.03.006.

[34] INGEOMINAS. Geología de la Plancha 18. Escala 1:100000, 2007.

[35] González, G., Mecanismo y profundidad de emplazamiento del Plutón de Cerro Cristales, Cordillera de la Costa, Antofagasta, Chile. Revista Geológica de Chile, 26, pp. 43-66, 1999. DOI: 0.4067/S0716-02081999000100003.

[36] Duque, J.F., Orozco, T., Cardona, A., Ferrari, L., Ruiz, J. y Valencia, V., El Batolito de Santa Marta, Colombia. Registro de la instalacion de una zona de subduccion Paleogena de la Placa Caribe bajo la Placa Samericana. Geos., 28(2). Sesión Regular: Geoquímica y Petrología. GEOQP-15 CARTEL, 2008.

[37] Bucher, K. and Frey, M., Petrogenesis of metamorphic rocks. 6ª ed., Complete revision of Winkler's textbook, Berlin Heidelberg, Springer-Verlag, 1994, 318 P.

[38] Bucher, K. and Grapes, R., Petrogenesis of Metamorphic Rocks. 8ª ed., Berlin Heidelberg, Springer-Verlag, 2002, 341P.

[39] Yardley, B.W.D. and Baltatzis, E., Retrogression of staurolite schists and the sources of infiltrating fluids during metamorphism. Contributions to Mineralogy and Petrology, 89, pp. 59-68, 1985. DOI: 10.1007/BF01177591.

[40] Ferry, J.M., Regional metamorphism of the Waits River formation, eastern Vermont: Delineation of a new type of giant hydrothermal system. Journal of Petrology, 33, pp. 45-94, 1992. DOI: 10.1093/petrology/33.1.45.

[41] Ague, J.J., Crustal mass transfer and index mineral growth in Barrow's garnet zone, northeast Scotland. Geology 25, pp. 73-76, 1997. DOI: 10.1130/0091-7613(1997)025<0073:CMTAIM>2.3.

[42] Oliver, N.H.S., Rubenach, M.J. and Valenta, R.K., Precambrian metamorphism, fluid flow, and metallogeny of Australia AGSO. Journal of Australian Geology & Geophysics, 17(4), pp. 31-53, 1998. DOI: 10.1016/S0024-4937(00)00021-9.

[43] Zharikov, V.A., Pertsev, N.N., Rusinov, V.L., Callegari, E. and Fettes, D.J., A systematic nomenclature for metamorphic rocks: 9. Metasomatic rocks. Recommendations by the IUGS Subcommission on the Systematics of Metamorphic Rocks. Recommendations, web version of 01.02.2007, 2007.

[44] Ardila, R., Carrascal, E.R. y Oyarzún, J., Proposición de un modelo genético para los yacimientos cupríferos tipo skarn de San Antonio y Panulcillo, Región de Coquimbo, Chile. En: VI Congreso Geológico Chileno, 1, pp. 256-260, 1991.

[45] Kenneth, Sh,. Mineralogical zoning in a Scapolite-Bearing Skarn body on San Gorgonio Mountain, California. American Mineralogist, 60, pp. 785-797, 1975.
[46] Cartwright, I. and Buick, I.S., Formation of wollastonite-bearing marbles during late regional metamorphic channelled fluid flow in the upper calcsilicate unit of the Reynolds Range group, central Australia. Journal of Metamorphic Geology, 13(3), pp. 397-417, 1995. DOI: 10.1111/j.1525-1314.1995.tb00228.x.
[47] Damman, A.H. and Kieft, C., W-Mo polymetallic mineralization and associated calcsilicate assemblages in the Gasborn area, West Bergslagen, Central Sweden. Canadian Mineralogist, 28, pp. 17-36, 1990.
[48] Del Lama, E.A., Candia, M.A.F. and Szabó, G.A.J., Petrography and metamorphism of the metasedimentary country-rocks of the Jacurici Valley Chromitite-Hosting mafic-ultramafic complexes, Bahia, Northeastern Brazil. Geologia USP. Série Científica, 1(1), pp. 1-15, 2001.
[49] Zaaboub, N., Abdeljaouad, S. and López-Galindo, A., Origin of fibrous clays in Tunisian Paleogene continental deposits. Journal of African Earth Sciences, 43(5), pp. 491-504, 2005. DOI: 10.1016/j.jafrearsci.2005.08.013.
[50] Merdhah, A.B.B. and Yassin, A.A.M., Laboratory Study on precipitation of Barium Sulphate in Malaysia sandstone cores. The Open Petroleum Engineering Journal, 2, pp. 1-11, 2009. DOI: 10.2174/1874834101002010001.
[51] Merdhah, A.B.B., Yassin, A.A.M. and Muherei, M.A., Laboratory and prediction of barium sulfate scaling at high-barium formation water. Journal of Petroleum Science and Engineering, 70, pp. 79-88, 2010. DOI: 10.1016/j.petrol.2009.10.001.
[52] Pertsev N.N., High temperature metamorphism and metasomatism of carbonate rocks. Nauka Publishing, Moscow, 1977.
[53] Grammatikopoulos, T.A. and Clarkb, A.H., A comparative study of wollastonite skarn genesis in the Central Metasedimentary Belt, southeastern Ontario, Canada. Ore Geology Reviews, 29(2), pp. 146-161, 2006. DOI: 10.1016/j.oregeorev.2005.11.007.
[54] Harris, N.B. and Einaudi, M.T., Skarn deposits in the Yerington district, Nevada: Metasomatic skarn evolution near Ludwig. Economic Geology, 77, pp. 877-898, 1982. DOI: 10.2113/gsecongeo.77.4.877.
[55] Pindell, J.L. and Barrett, S.F., Geological evolution of the Caribbean region: A plate-tectonic perspective. In: Dengo, G. and Case, J.E., Eds., The Caribbean region, The Geology of North America, H, Geological Society of America, 1990, pp. 405-432.
[56] Pindell, J.L., Regional synopsis of Gulf of Mexico and Caribbean evolution: Gulf coast section, Society for Sedimentary Geology, 13th Annual Research Conference Proceedings, 1993, pp. 251-274.
[57] Vinasco, C., Cordani, U., González, H., Weber, M. and Peláez, C., Geochronological, isotopic and geochemical data from Permo-Triassic granitic gneisses and granitoids of the Colombian Central Andes. Journal of South American Earth Sciences, 21, pp. 355-371, 2006. DOI: 10.1016/j.jsames.2006.07.007.
[58] Ayala, R.C., Bayona, G., Cardona, A., Ojeda, C., Montenegro, O.C., Montes, C., Valencia, V. and Jaramillo, C., The paleogene synorogenic succession in the northwestern Maracaibo block: Tracking intraplate uplifts and changes in sediment delivery systems. Journal of South American Earth Sciences, 39, pp. 93-111, 2012. DOI: 10.1016/j.jsames.2012.04.005.

O.M. Castellanos-Alarcón, received his BSc in Geology in 1999 from the Universidad Industrial de Santander, Colombia. He was awarded an MSc in Geology in 2001 from the Shimane University, Japan. He has been working as a full-time Lecturer on the Geology Program, Universidad de Pamplona, Colombia, since 2003. He is specialist in mineralogy, experimental mineralogy, petrology and geochemistry of metamorphic rocks.
ORCID: 0000-0003-0620-0540.

C.A. Ríos-Reyes, received his BSc in Geology in 1989 and his Post-graduate Diploma in University Teaching in 1995 from the Universidad Industrial de Santander, Colombia. He was awarded an MSc in Geology from the Shimane University, Japan, in 1999. He was awarded a PhD in Applied Sciences from the University of Wolverhampton, England, in 2008. He has been working as a full-time Lecturer of the School of Geology, Universidad Industrial de Santander, Colombia, since 1992, He is a specialist in mineralogy, experimental and environmental mineralogy, petrology and geochemistry of metamorphic rocks.
ORCID: 0000-0002-3508-0771.

L.C. Mantilla-Figueroa, received his BSc in Geology in 1987 and his MSc in Mineralogical Sciences in 1989 from the Moscow Geological Prospecting Sergo Odzhinikidze Institute, Russia. He was awarded his PhD in Petrology and Geochemistry in 1999 from the Universidad Complutense de Madrid, Spain. Recently, he has undertaken a postdoctoral research in Metallogeny at the University of British Columbia, Canada. He has been working as a full-time Lecturer in the School of Geology, Universidad Industrial de Santander, Colombia, since 1993. He is a specialist in the petrology and geochemistry of igneous and metamorphic rocks, regional geology, process fluid-rock interaction, and exploration of mineral deposits.
ORCID: 0000-0002-2112-8041.